



ELSEVIER

Physica D 109 (1997) 24–31

**PHYSICA D**

## Particle propagation in a random and quasi-periodic potential

F. Borgonovi<sup>a,1</sup>, D.L. Shepelyansky<sup>b,\*</sup><sup>a</sup> *Dipartimento di Matematica, Università Cattolica, via Trieste 17, 25121 Brescia, Italy*<sup>b</sup> *Laboratoire de Physique Quantique, UMR C5626 du CNRS, Université Paul Sabatier, 31062 Toulouse Cedex, France*

### Abstract

We numerically investigate the Anderson transition in an effective dimension  $d$  ( $3 \leq d \leq 11$ ) for one particle propagation in a model random and quasi-periodic potential. The found critical exponents are different from the standard scaling picture. We discuss possible reasons for this difference.

PACS: 71.55.Jv; 05.45.+b

The Anderson transition has been intensively investigated during last years. According to the scaling theory for spinless particles all states are localized for dimension  $d \leq 2$ , while a transition from localization to diffusive propagation occurs for  $d > 2$  when a certain hopping parameter  $k$  crosses a critical value  $k_{cr}$  (see reviews [1,2]). The one parameter scaling theory predicts that in the localized phase ( $k < k_{cr}$ ) the typical localization length of wavefunctions diverges at the critical point as  $l \sim |k - k_{cr}|^{-\nu}$ . Above the critical point the dynamics is diffusive and the DC conductivity  $\sigma$  which is proportional to the diffusion rate  $D$  is assumed to approach zero at the critical point as  $\sigma \propto D \sim |k - k_{cr}|^s$ . Scaling arguments give the following relation between the exponents:  $s = (d - 2)\nu$ . For dimension  $d = 2 + \epsilon$  the  $\epsilon$  expansion theory predicts  $s = \nu = 1 + O(\epsilon^4)$  [3]. In

higher dimensions the problem was studied by many authors [4–6]. According to the results presented there  $\nu = 1/2$  for  $d \rightarrow \infty$  while for the delocalized phase  $s \approx d/2$  [6] or  $\sigma$  decreases exponentially near the transition [4].

Numerical investigations of the exponents has been restricted to  $d = 3$  where it was found  $s = \nu = 1.5 \pm 0.1$  ([2] and reference therein) in agreement with the scaling relation between  $\nu$  and  $s$ . However, the applied numerical methods were quite heavy and did not allow to obtain a better accuracy in the determination of the exponents or to increase the dimension. For  $2 < d \leq 3$  and  $d = 4$  there are only recent results for  $\nu$  [7] obtained by transfer matrix technique. While the results there seem to be in agreement with the scaling theory the system size was so small that the question if the thermodynamic limit had been reached remains open.

An effective way to increase the number of dimensions was proposed in [8] and applied for investigation of transition in  $d = 3$  [9] where it was also found  $s \approx 1.25$  and  $\nu \approx 1.5$ . The method consists in the investigation of the well-known model of quantum chaos

\* Corresponding author. Also at: Budker Institute of Nuclear Physics, 630090 Novosibirsk, Russian Federation.

<sup>1</sup> Also at: Istituto Nazionale di Fisica della Materia, Unità di Milano, via Celoria 16, 22100 Milano, Italy and Istituto Nazionale di Fisica Nucleare, sezione di Pavia, via Bassi 7, 2700 Pavia, Italy.

namely the kicked rotator model with a frequency-modulated amplitude of kicks. The time-dependent Hamiltonian of the model is given by

$$H = H_0(\hat{n}) + V(\theta, t)\delta_1(t), \quad (1)$$

where  $\delta_1(t)$  is the periodic delta function with period 1 between kicks,  $\hat{n} = -i\partial/\partial\theta$  and  $\theta$  is a periodic angle variable.  $H_0$  determines the spectrum of unperturbed energies  $E_n$  chosen randomly distributed in  $(0, 2\pi)$ . The perturbation  $V$  depends on time in a quasi-periodic way:

$$V(\theta, t) = -2 \tan^{-1} \left( 2k \left( \cos\theta + \sum_{j=1}^{d-1} \cos(\theta_j + \omega_j t) \right) \right) \quad (2)$$

with  $d - 1$  incommensurate frequencies  $\omega_j$ . Here  $\theta_j$  are initial phases and the time is measured in number of kicks. The Hamiltonian (1) can be re-written in the extended phase space by letting  $\hat{n}_j = -i\partial/\partial\theta_j$ . After that the problem becomes periodic in time and the eigenvalues equation for the quasi-energy eigenfunctions can be mapped to the usual solid-state form [9,10]:

$$T_{\mathbf{n}} u_{\mathbf{n}} + k \sum_{\mathbf{r}}' u_{\mathbf{n}-\mathbf{r}} = 0, \quad (3)$$

where the  $\sum'$  indicates a sum over the nearest neighbors to  $\mathbf{n}$  on a  $d$ -dimensional lattice and the diagonal term at the site  $\mathbf{n} = (n, n_1, \dots, n_j, \dots, n_{d-1})$  is

$$T_{\mathbf{n}} = -\tan \left( \frac{1}{2} \left( E_n + \sum_{j=1}^{d-1} \phi_j + \lambda \right) \right). \quad (4)$$

Here  $\phi_j = n_j \omega_j$  and  $\lambda$  is the quasi-energy. If  $\phi_j$  are randomly distributed in  $(0, 2\pi)$  then Eq. (3) becomes equivalent to the Lloyd model at the center of the band ( $E = 0$ ). The parameter  $\lambda$  determines only the phase shift and it is clear that the physical characteristics are independent on its value. Since the mapping between (1) and (3) is exact, it is possible to study the Anderson transition in  $d$ -dimensions by investigating the dynamics of the one-dimensional system (1). This gives an effective gain of order  $N^{d-1}$  in numerical computations if  $N$  is the system size. Finally, discussing the

model, we should mention that the presence of disorder in the expression for  $T_{\mathbf{n}}$  is crucial. Indeed, according to the exact mathematical results [11] in the case of pure quasi-periodic potential when in (4)  $E_n = \omega n$  all states for typical irrational frequencies are exponentially localized for any  $d$  (for 1D case see also [12]). The physical meaning of this result is quite clear: the classical dynamics in this case is integrable and variation of unperturbed actions (levels  $\mathbf{n}$ ) is restricted by invariant curves. However, even if only in one direction the dispersion becomes nonlinear (e.g.  $E_n \propto n^2$ ) then the classical dynamics can become chaotic with diffusive spreading in all  $\mathbf{n}$  directions. In this paper we investigate how this diffusion is affected by quantum effects. For simplicity we study the case with random variation of  $E_n$  with  $n$ , which is also nonlinear.

Using the above approach we studied numerically the Anderson transition for integer  $3 \leq d \leq 11$  in the model (1) and (2). The choice of frequencies was the following: for  $d = 3$  we fixed  $\omega_{1,2}/2\pi = 1/\lambda, 1/\lambda^2$  with  $\lambda = 1.3247, \dots$  being the real root of the cubic equation  $x^3 - x - 1 = 0$  which gives the most irrational pair [9]; for  $d = 4$  we added  $\omega_3/2\pi = 1/\sqrt{2}$  and for  $d > 4$  we chose all frequencies randomly in the interval  $(0, 2\pi)$ . The size of the basis  $N$  was between 1024 and 4096. The total number of iterations (kicks) was usually around  $10^6$  but in some cases close to the critical point the evolution was followed up to  $10^7$  kicks. We used from 10 to 100 realizations of disorder to suppress statistical fluctuations.

A typical example of diffusive spreading over the lattice for  $d = 4$  is shown in Fig. 1. Here  $k > k_{cr}$  and the second moment of the probability distribution grows linearly with time. At the same time the probability distribution over levels has the gaussian shape (see Fig. 1(b)). This allows to determine the diffusion constant  $D$ . Usually, we extract it from the probability distribution since here the statistical fluctuations are lower than for the value obtained from the second moment  $D = n^2/t$ . However, both methods give quite close values. The value of  $D$  found in this way is then averaged over different realizations of disorder. For  $k < k_{cr}$  the probability distribution averaged in time reaches a stationary exponentially localized form and at the same time the growth of the second moment  $n^2$

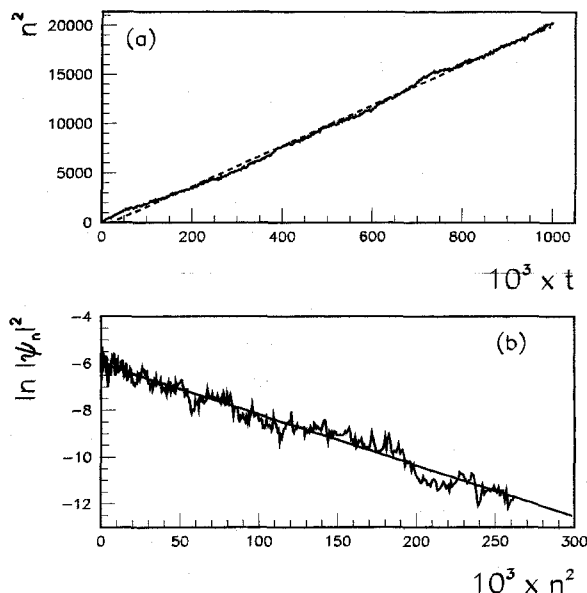


Fig. 1. (a) Behavior of the second moment on time for  $k = 0.33$ ,  $d = 4$  (diffusive side). Dashed line is the fitted diffusion coefficient  $D = 0.0205$ . Fourier basis is  $N = 1024$ . (b) Logarithm of the averaged distribution function between  $t = 0.995 \times 10^6$  and  $t = 10^6$  ( $t =$  number of kicks). Full line is the best fit gaussian which gives a diffusion coefficient  $D = 0.0229$ . On  $x$ -axis we put  $n^2$ .

is saturated (Fig. 2). From the obtained stationary distribution the localization length is determined in two ways. One is by the square list fitting of  $\ln |\psi_n|^2 = -2\gamma n + b$  with the localization length being  $l = 1/\gamma$  and  $b$  some constant.<sup>2</sup> Another definition is via the participation ratio so that  $\gamma_i = \sum_n |\psi_n|^4 / \sum_n |\psi_n|^2$ . After that both values  $\gamma$  and  $\gamma_i$  were averaged over different realizations of disorder. The inverse participation ratio  $1/\gamma_i$  determines another length scale which in principle can be parametrically different from  $l$ .

The numerical results for the dependence of  $D$ ,  $\gamma$  and  $\gamma_i$  on parameter  $k$  for the effective dimension  $d =$

<sup>2</sup>Let us mention that in [9] it was chosen  $b = \ln \gamma$  to have normalization equal to one. This choice enhances the contribution of the states near the maximum at  $n = 0$  so that  $\gamma$  defined in this way becomes close to the definition of  $\gamma$  via the participation ratio  $\gamma_i$ . For  $d = 3$  our data for  $\nu(\gamma_i)$  defined via  $\gamma_i$  give (see Table 1)  $\nu(\gamma_i) = 1.71(6)$  to be compared with  $\nu \approx 1.5$  from [9]. The fit without fixing  $b$  stress more the contribution of far exponential tails where according to our data the exponent is larger  $\nu(\gamma) = 2.37(1)$ .

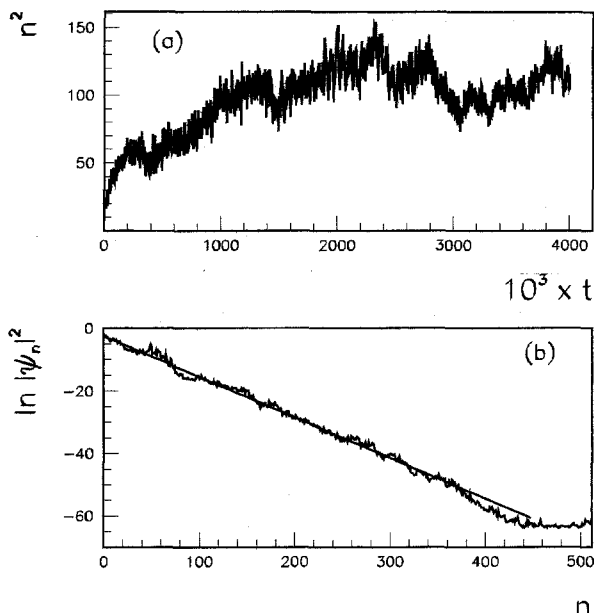


Fig. 2. (a) Behavior of the second moment on time for  $k = 0.24$ ,  $d = 4$  (localized side). Basis is  $N = 1024$ . (b) Logarithm of the averaged distribution function between  $t = 0.3995 \times 10^7$  and  $t = 0.4 \cdot 10^7$ . On  $x$ -axis we put  $n$ . Line represents the fitted localized distribution with  $l = 15.4$ .

3 are presented in Figs. 3 and 4. To determine the scaling near the critical point we used the three parameter fit of the type  $\gamma_{(i)} = \gamma_0 |k - k_{cr}|^\nu$  and  $D = D_0 |k - k_{cr}|^s$ . The results of the fitting are given in the figure captions (see also Table 1) as well as the parameters of  $\chi^2$  test. Formally the statistical error of the exponents  $s, \nu$  found in this way is rather small (less than 1% of the value). However, the estimate of non-statistical errors is quite difficult since the fitting procedure is rather sensitive to the value of  $k_{cr}$ . From comparison of  $k_{cr}$  values obtained from diffusive and localized phases it can be estimated on the level of 5%. The values of the exponents for  $D$  and  $\gamma_i$  are in good agreement with the results of [9] (see also footnote 2). Our data indicate significant difference for the exponents  $\nu$  defined via  $\gamma$  and  $\gamma_i$  for  $d = 3$ . To demonstrate the dependence near the critical point we fixed the value of  $k_{cr}$  defined from Fig. 3 and show the behavior in log-log scale near  $k_{cr}$  in Fig. 4. The two parameter fit with fixed  $k_{cr}$  shown in Fig. 4 gives similar values of the exponents  $s, \nu$  as in the case of Fig. 3. The linear

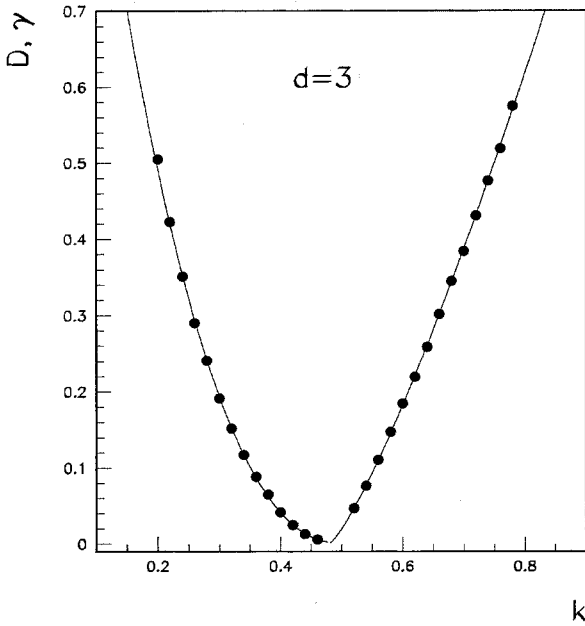


Fig. 3. Inverse localization length (left side) and diffusion rate (right side) for  $d = 3$ . Lines are the separate fits:  $\gamma = \gamma_0(k_{cr} - k)^\nu$  with  $\gamma_0 = 8.01$  (1),  $k_{cr} = 0.509$  (1) and  $\nu = 2.37$  (1) with  $\chi^2 = 10.5$  and  $D = D_0(k - k_{cr})^s$  with  $D_0 = 2.56$  (2),  $k_{cr} = 0.479$  (1) and  $s = 1.25$  (1) with  $\chi^2 = 32.6$ . A similar fit for  $\gamma_i = \gamma_{0i}(k_{cr} - k)^{\nu_i}$  gives  $\gamma_{0i} = 3.7$  (3),  $k_{cr} = 0.489$  (4),  $\nu_i = 1.71$  (6) and  $\chi^2 = 15.4$ . Here 10–100 random configurations have been iterated up to  $10^7$  kicks. Data errors are within the symbol size.

dependence of  $\ln \gamma$ ,  $\ln D$  on  $\ln |1 - k/k_{cr}|$  describes quite well the variation of localization length and diffusion in one/two orders of magnitude.

The case with the dimension  $d = 4$  was investigated in a similar way. The results are presented in Figs. 5 and 6. They definitely show stronger deviation from the scaling relation between exponents  $\nu$ ,  $s$ . Especially pronounced is the small value of  $s$  which remains less than 2.

In spite of this deviation from the scaling relation the behavior at the critical point is close to the standard expectations [1–6]. Indeed, at  $k_{cr}$  the conductance has a finite critical value  $g^*$ . From another side  $g \sim E_c/\Delta$  where  $E_c \sim D/L^2$  is the Thouless energy,  $D$  the diffusion coefficient and  $\Delta \sim B/L^d$  is the level spacing in a block of size  $L$  with  $B \sim 1$  being the band width. Therefore, at  $k_{cr}$  one has  $D \sim Bg^*/R^{d-2}$  where  $R \sim L$  is a typical length scale. At

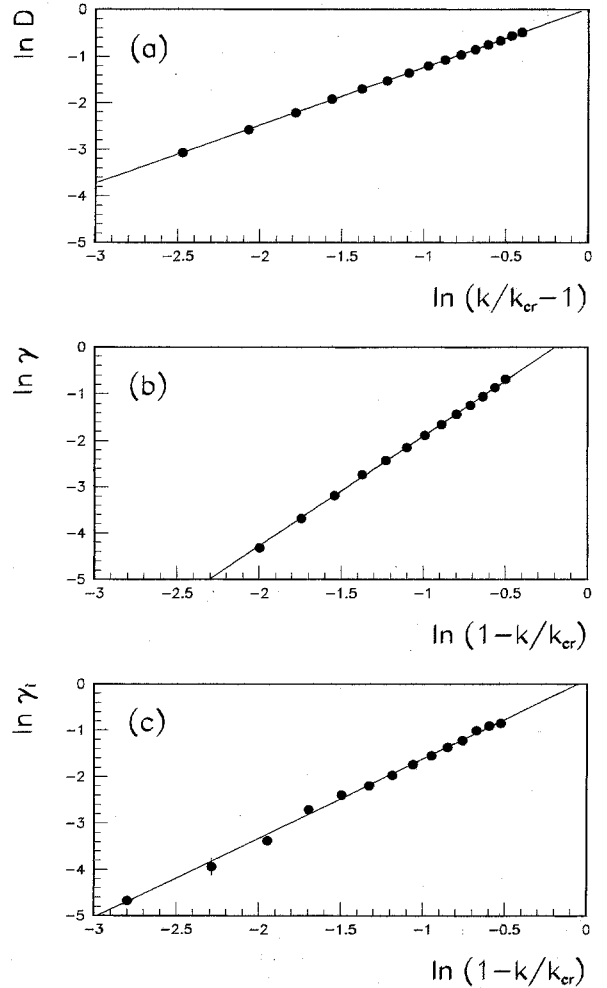


Fig. 4.  $d = 3$ . (a) Logarithm of diffusion rate vs.  $\ln(k/k_{cr} - 1)$  where  $k_{cr}$  is extracted from the separate fit (Fig. 3). Straight line is the best fit line with slope  $s = 1.248$  (5) and  $\chi^2 = 10.6$ . (b) Logarithm of the inverse localization length vs.  $\ln(1 - k/k_{cr})$  where  $k_{cr}$  is extracted from the separate fit (Fig. 3). Straight line is the best fit line with slope  $\nu = 2.374$  (9) and  $\chi^2 = 33.8$ . (c) Logarithm of the participation ratio  $\gamma_i$  vs.  $\ln(1 - k/k_{cr})$  where  $k_{cr} = 0.489$  (4) is extracted in a similar way from a three parameter fit. Here the straight line has slope  $\nu_i = 1.71$  (6) and  $\chi^2 = 16.3$ . Here 10–100 random configurations have been iterated up to  $10^7$  kicks. Errors are within the symbol size.

the same time  $D = R^2/t$  so that finally  $R^d \sim Bg^*t$ . Our numerical data for the values of  $k$  close to  $k_{cr}$  (Figs. 7 and 8 show that this relation works. Formal fits give  $R^d \sim t^\alpha$  with  $\alpha = 1.13$  ( $d = 3$ ),  $1.12$  ( $d = 4$ ) close to the expected value. We also analyzed the decay of the average probability to stay at the origin

Table 1

| $d$ | $s$      | $\nu(\gamma_i)$ | $(d-2)\nu(\gamma_i) - s$ | $\nu(\gamma)$ | $(d-2)\nu(\gamma) - s$ |
|-----|----------|-----------------|--------------------------|---------------|------------------------|
| 3   | 1.25 (1) | 1.71 (6)        | 0.46                     | 2.37 (1)      | 1.12                   |
| 4   | 1.52 (5) | 2.59 (2)        | 3.66                     | 2.53 (1)      | 3.54                   |
| 5   | 2.04 (3) | –               | –                        | 2.32          | 4.92                   |
| 11  | 1.87 (1) | –               | –                        | 2.55          | 21.0                   |

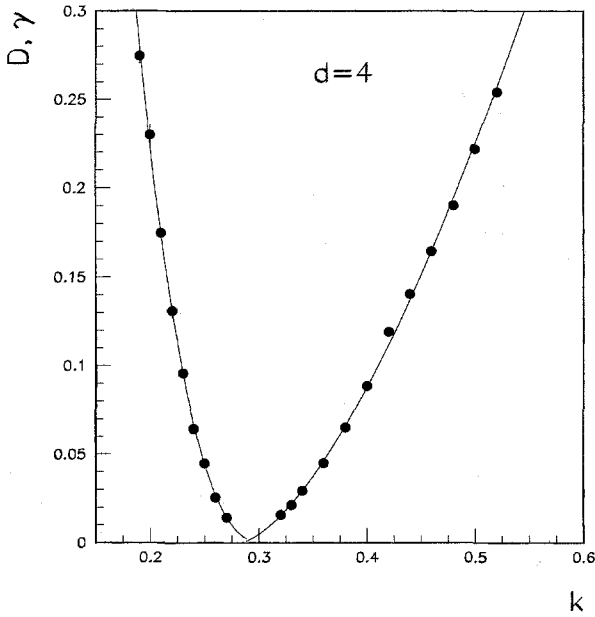


Fig. 5. Inverse localization length (left side) and diffusion rate (right side) for  $d = 4$ . Lines are the separate fits:  $\gamma = \gamma_0(k_{\text{cr}} - k)^\nu$  with  $\gamma_0 = 66$  (10),  $k_{\text{cr}} = 0.306$  (2) and  $\nu = 2.53$  (1) with  $\chi^2 = 10.2$  and  $D = D_0(k - k_{\text{cr}})^s$  with  $D_0 = 2.29$  (2),  $k_{\text{cr}} = 0.283$  (3) and  $s = 1.52$  (5) with  $\chi^2 = 111$ . A similar fit for  $\gamma_i = \gamma_{0i}(k_{\text{cr}} - k)^{\nu_i}$  gives  $\gamma_{0i} = 85$  (28),  $k_{\text{cr}} = 0.305$  (5),  $\nu_i = 2.59$  (2) and  $\chi^2 = 4.5$ . Here 10–100 random configurations have been iterated up to  $10^7$  kicks. Data errors are within the symbol size.

$n_0$ :  $P_0(T) = (1/T) \int_0^T dt |\psi_{n_0}(t)|^2$ . As can be seen in Figs. 7(b) and 8(b) it is characterized by a power law decay. The numerically obtained values of the power are not far from  $1/d$  (Figs. 7 and 8). This indicates that multifractal exponents are relatively small. This fact is also confirmed by the rescaling of the probability distribution  $f_n = |\psi_n|^2$  at different moments of time (Fig. 9). It shows that after rescaling  $t^{1/d} f_n$  and  $n/t^{1/d}$  the distribution remains approximately stationary in time.

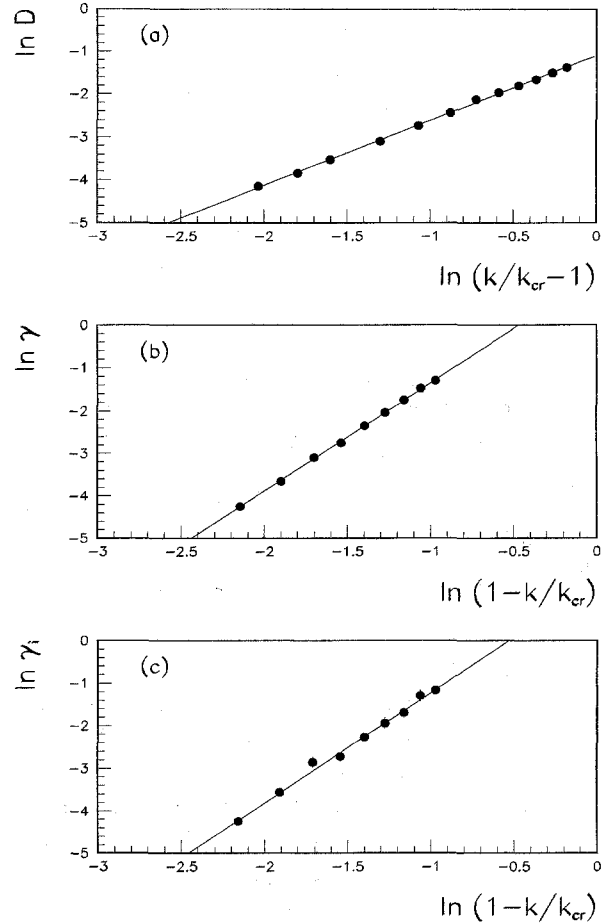


Fig. 6.  $d = 4$ . (a) Logarithm of diffusion rate vs.  $\ln(k/k_{\text{cr}} - 1)$  where  $k_{\text{cr}}$  is extracted from the separate fit (Fig. 5). Straight line is the best fit line with slope  $s = 1.519$  (4) and  $\chi^2 = 115$ . (b) Logarithm of the inverse localization length vs.  $\ln(1 - k/k_{\text{cr}})$  where  $k_{\text{cr}}$  is extracted from the separate fit (Fig. 5). Straight line is the best fit line with slope  $\nu = 2.534$  (5) and  $\chi^2 = 91.81$ . (c) Logarithm of the participation ratio  $\gamma_i$  vs.  $\ln(1 - k/k_{\text{cr}})$  where  $k_{\text{cr}} = 0.305$  (5) is extracted in a similar way from a three parameter fit. Here the straight line has slope  $\nu_i = 2.59$  (2) and  $\chi^2 = 4.5$ . Here 10–100 random configurations have been iterated up to  $10^7$  kicks. Errors are within the symbol size.

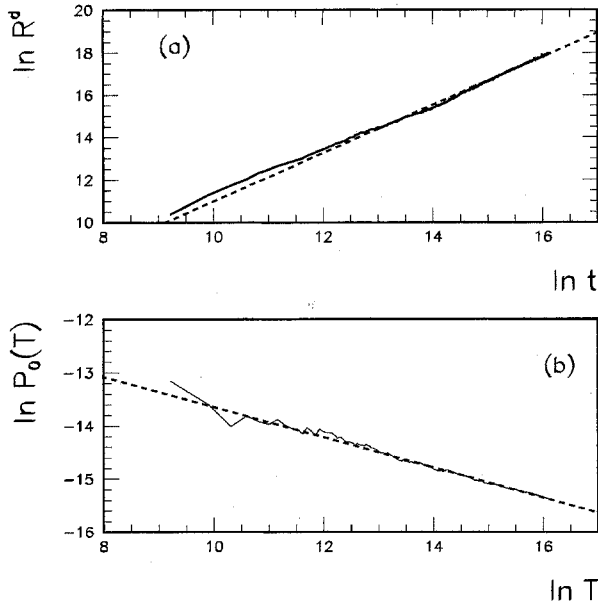


Fig. 7.  $d = 3$ . Study near the critical point at  $k = 0.48$ . (a) Behavior of  $R^d = \sum_n |n|^d |\psi_n|^2$  in time. Best fit (dashed line) gives  $R^d \sim t^{1.13(3)}$ . (b) Behavior of the logarithm of the integrated probability to stay  $P_0(T)$  as a function of the logarithm of time  $T$ . Here is  $P_0(T) = (1/T) \int_0^T dt |\psi_{n_0}(t)|^2$  and the initial state vector is  $\psi(t=0) = \delta_{n,n_0}$ . Best fit (dashed line) gives  $P_0(T) \sim T^{-0.28(3)}$ . One random configuration has been considered. Basis is  $N = 4096$ .

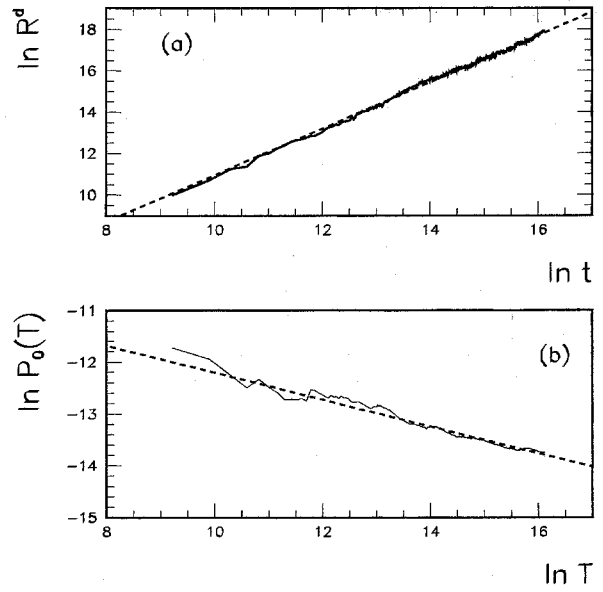


Fig. 8. The same as Fig. 7 but for  $d = 4$  near the critical point at  $k = 0.27$ . Results from fit gives  $R^d \sim t^{1.12(3)}$  and  $P_0(T) \sim T^{-0.26(3)}$ .

We also investigated the delocalization transition for  $d = 5, 11$  (Figs. 10 and 11). From the localized side the transition was very sharp (very large  $\gamma_0$ ) and it is not clear how accurate are the critical exponents obtained in this region even if the formal statistical error is quite small. Namely, the fits for  $\gamma$  in the localized phase give  $\gamma_0 = 257$  (28),  $k_{cr} = 0.214$  (1),  $\nu = 2.32$  (4) with  $\chi^2 = 0.18$  at  $d = 5$  and  $\gamma_0 = 2115$  (181),  $k_{cr} = 0.107$  (2),  $\nu = 2.55$  (2) with  $\chi^2 = 0.04$  at  $d = 11$ . However, from the diffusive side the transition is going in a rather smooth way with the exponent  $s$  close to 2 being quite different from the expectations of scaling theory (see Figs. 10 and 11). The values of the exponents for different dimensions are presented in Table 1. It definitely shows that the scaling relation  $s = (d-2)\nu$  does not work at all. Contrary to that our numerical data indicate that for  $d \gg 1$  the exponent  $s$  approaches to its limiting value  $s \approx 2$ .

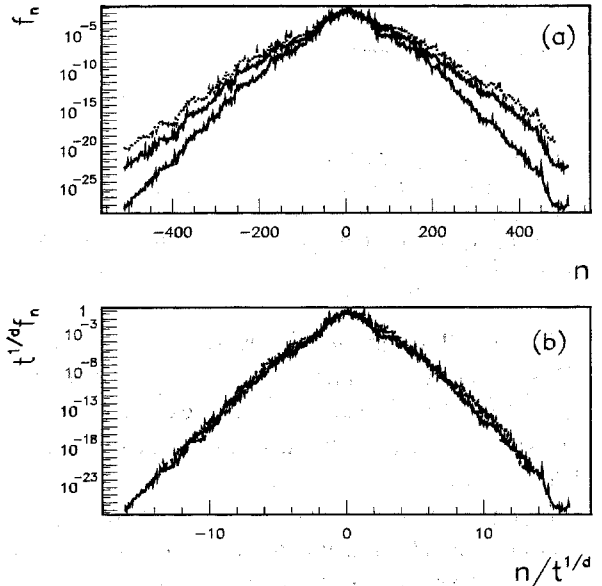


Fig. 9. Rescaling of the distribution function in the critical region ( $k = 0.27$ ) for  $d = 4$ . (a) The averaged (over  $10^4$  kicks) probability distribution over the unperturbed basis  $f_n$  taken at three different times  $t_1, 2t_1, 3t_1$  where  $t_1 = 10^6$ , shows that as the time goes on the distribution increases its size. (b) The same as (a) but in the rescaled variables  $t^{1/d} f_n$  and  $n/t^{1/d}$  (since at the critical point  $|n|^d \sim t$  with  $d = 4$ ).

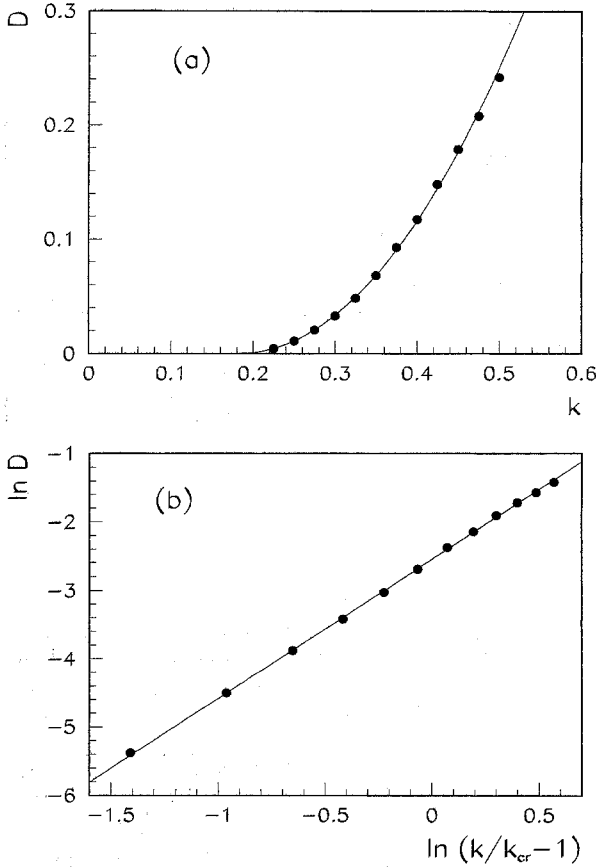


Fig. 10.  $d = 5$ . (a) Diffusion rate vs.  $k$ , three parameters fit (full line) gives:  $D = 2.56$  (6)  $(k - 0.180$  (2)) $^{2.04}$  (3) with  $\chi^2 = 36.1$ ; (b) logarithm of diffusion rate vs.  $\ln(k/k_{cr} - 1)$  where  $k_{cr}$  is extracted from (a). Best fit (full line) has the slope  $s = 2.039$  (9).

In Fig. 12 we show the dependence of  $k_{cr}$  on  $d$  which scales approximately as  $1/d$  in high dimensions. This type of behavior can be expected since in the kick potential all frequencies are mixed only if  $k \sum_{j=1}^d \cos(\omega_j t) \sim k_{cr} d \sim 1$ .

In conclusion, we studied the Anderson transition in a model random and quasi-periodic potential with effective dimension  $d \geq 3$ . This model demonstrates quite many features which are the same as for the standard Anderson transition in a disordered  $d$ -dimensional potential. For  $d = 2$  all states are localized and the localization length grows exponentially with the decrease of disorder [8]. For  $d = 3$  the model has a transition from localization to diffusion with

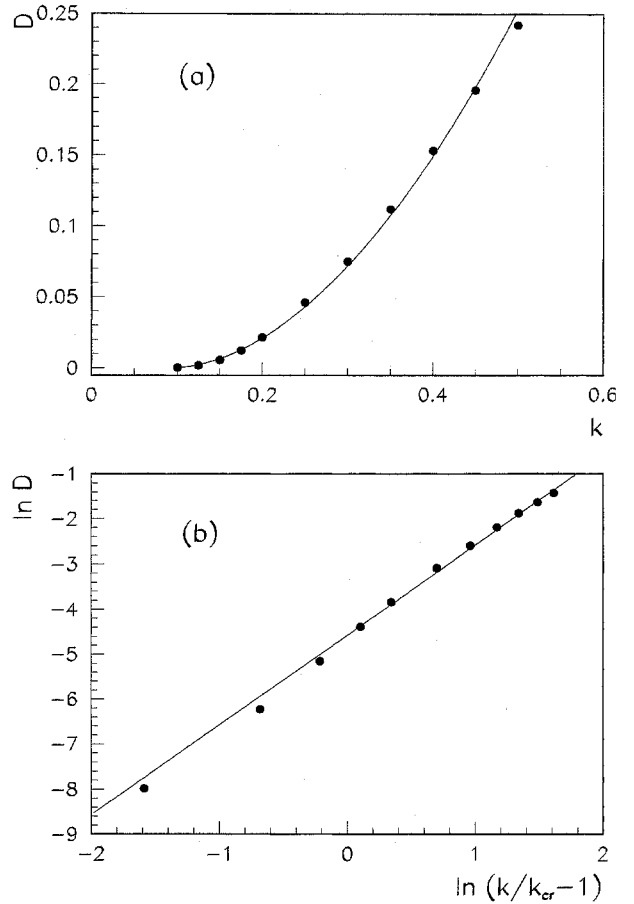


Fig. 11.  $d = 11$ . (a) Diffusion rate vs.  $k$ , three parameters fit gives:  $D = 1.35$  (1)  $(k - 0.0924$  (5)) $^{1.87}$  (1) with  $\chi^2 = 310$ ; (b) logarithm of diffusion rate vs.  $\ln(k/k_{cr} - 1)$  where  $k_{cr}$  is extracted from (a). Best fit (full line) has the slope  $s = 1.99$  (5).

the critical exponents close to expected [9]. However, for higher dimensions the exponents strongly deviate from the expected scaling relation  $s = (d - 2)\nu$ . Contrary to that our numerical data show that for  $d \gg 1$  one has  $s \approx 2$ . It is possible to give the following argument supporting  $s = 2$ . For  $d \gg 1$  the critical value of the coupling goes to zero  $k_{cr} \sim 1/d$ . Therefore, the change of action is governed by the equation

$$\partial n / \partial t \approx k \cos \theta \sum_{j=1}^d \cos \omega_j t. \quad (5)$$

For  $d$  going to infinity this sum gives the real diffusive process in which  $n^2 \sim k^2 t \sim Dt$ . Due to that it

is in some sense natural to expect that asymptotically for  $d \gg 1$  the exponent  $s$  approaches to 2. This is in agreement with our numerical data where  $D$  varied by 2–3 orders of magnitude near the critical point (see e.g. Figs. 10 and 11). However, further investigations are required to conclude whether the behavior of the scaling exponents is a peculiarity of the model under investigation. Indeed, in our model there are some correlations between hyperplanes with the same value of  $n$ . However, in our opinion for the classical model chaos and diffusion in all directions can appear even if the motion is nonlinear only in one direction ( $E_n$  changes with  $n$  in a nonlinear way or randomly). Due to that we think that the quantum dynamics of the above model should be quite similar to a real disordered system in dimension  $d$ .

### Acknowledgements

We thank V. Kravtsov for useful discussions. One of us (FB) is very grateful to the Laboratoire de Physique Quantique, UMR C5626 du CNRS, University P. Sabatier, for the hospitality extended to him during his visit when this work had been started and

another (DLS) thanks the University at Como for hospitality during different stages of this work.

### References

- [1] P.A. Lee and T.V. Ramakrishnan, *Rev. Mod. Phys.* 57 (1985) 287; in: *Anderson Localization*, eds. Y. Nagaoka and H. Fukuyama, Springer Ser. Solid in Solid State Sci. 39 (Berlin, 1982).
- [2] B. Kramer and A. MacKinnon, *Rep. Prog. Phys.* 56 (1993) 1469.
- [3] S. Hikami, *Nucl. Phys. B* 215 (1986) 555.
- [4] K.B. Efetov and O. Vichweger, *Phys. Rev. B* 45 (1992) 11546.
- [5] M.R. Zirnbauer, *Phys. Rev. B* 34 (1986) 6394; *Nucl. Phys. B* 265 (1986) 375.
- [6] A.D. Mirlin and Y.V. Fyodorov, *Phys. Rev. Lett.* 72 (1994) 526; *J. Phys. France* 4 (1994) 665.
- [7] M. Schreiber and H. Grussbach, *Phys. Rev. Lett.* 76 (1996) 1687.
- [8] D.L. Shepelyansky, *Physica D* 8 (1983) 208.
- [9] G. Casati, I. Guarneri and D.L. Shepelyansky, *Phys. Rev. Lett.* 62 (1989) 345.
- [10] S. Fishman, in: *Quantum Chaos*, eds. G. Casati, I. Guarneri and U. Smilansky (North-Holland, Amsterdam, 1993) p. 187.
- [11] J. Bellissard, R. Lima and E. Scoppola, *Commun. Math. Phys.* 88 (1983) 465; L.A. Pastur and A.L. Figotin, *Pis'ma ZhETF* 37 (1983) 575.
- [12] M.V. Berry, *Physica D* 10 (1984) 369.